Controller Design in a Fuel-Cell Powered Automobile

Srinivas Palanki[a] [1] **John C. Telotte**[b]

[a] *Department of Chemical and Biomolecular Engineering, University of South Alabama, Mobile, AL 36688, USA*
[b] *Department of Chemical and Biomedical Engineering, Florida State University, Tallahassee, FL 32310-6046, USA*

Abstract: In this paper, the control problems that arise during dynamic operation of a fuel-cell powered automobile, are analyzed. In particular, it is shown that there are three distinct control problems that need to be solved when the power demand fluctuates. A logic-based switching controller is proposed that switches to the battery backup when the fuel cell is unable to provide the necessary power to the motor. An adaptive controller is developed based on a linear model that adjusts the hydrogen flow into the fuel cell in response to changing power demand. Finally, a thermal controller is developed based on a nonlinear model that regulates the temperature of the fuel cell. Interaction between these controllers is analyzed via simulations under realistic road conditions.

Keywords: controller design, PEM fuel cell, automotive power generation system

1. INTRODUCTION

Fuel cell power systems for automotive applications have received increased attention in recent years because of their potential for high fuel efficiency and lower emissions [Zalc and Loffler, 2002]. While there have been significant advances in fuel cell technology, one reason this technology has not seen wide-spread applications in the automotive industry has been the lack of an efficient hydrogen distribution center and the difficulties associated with storing hydrogen onboard an automobile. One option to alleviate these problems is to develop a system that utilizes a commonly available carbon-based hydrogenous fuel such as gasoline or methane to generate the necessary hydrogen *in situ* on an "as needed" basis. In this paper, we identify three separate control problems that need to be solved in a fuel-cell powered automobile.

2. SYSTEM DESIGN CONSIDERATIONS

A schematic of the fuel cell system under consideration is shown in Fig. 1. The two main components of the overall system are (1) the fuel processing subsystem and (2) the power generation subsystem. Methane enters the fuel processing subsystem and is converted to hydrogen. Hydrogen enters the fuel cell where it mixes with oxygen to generate electrical power which drives an electric motor. In addition to the fuel cell, there is a battery backup that the electric motor switches to when the hydrogen delivered to the fuel cell is insufficient to meet the *instantaneous* power demands of the electric motor. This battery backup is essential because significant load transitions occur frequently as a result of sudden acceleration on highway ramps as well as terrain changes [Zalc and Loffler, 2002].

[1] Corresponding author: palanki@usouthal.edu

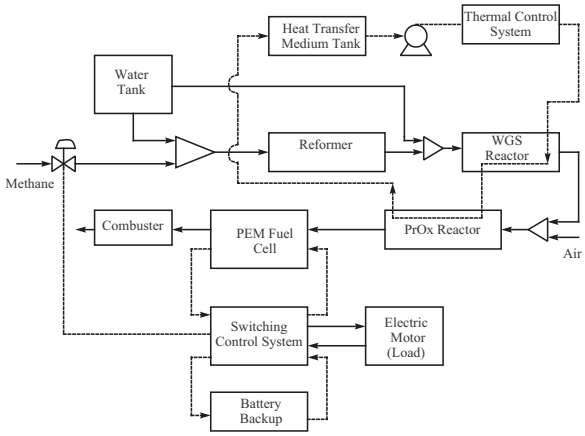

Fig. 1. Schematic of Fuel Cell System

In an earlier paper [Kolavennu *et al.*, 2006], the primary components of a fuel cell power system, that utilizes methane to generate hydrogen, were analyzed. In particular, basic chemical engineering principles were utilized to design a reactor train that converts methane to hydrogen of the desired purity. The relation between power produced by a PEM fuel cell and methane entering the reactor train *at steady state* was calculated. However, a typical automobile does not operate at steady state. The power demand for an automobile motor undergoes significant variations due to acceleration, changes in road surface and traffic conditions.

In this paper, we analyze the control problems that arise during dynamic operation of a fuel-cell powered automobile in the face of fluctuating power demand. In particular, it is shown that there are three distinct control problems that need to be solved when the power demand fluctuates. When power demand goes down, the excess hydrogen can

be diverted from the fuel cell. A sudden *increase* in power demand requires an instantaneous increase in hydrogen flow rate into the fuel cell. However, the conversion of methane to hydrogen takes several seconds which leads to an unacceptable lag between power demand of the motor and the power supplied by the fuel cell. For this reason, a backup battery is required that takes over this power load during the time it takes for the fuel cell to generate the necessary power and a suitable controller is required that switches between the fuel cell and the battery backup. If sufficient hydrogen is being produced by the fuel processor, a separate controller is required to adjust the hydrogen flow into the fuel cell in response to changing power demand. Finally, the fuel cell is subject to temperature changes and a thermal controller is required to regulate the temperature to the desired setting. In the paper, we propose the following controllers:

- A logic-based switching controller that switches to the battery backup when the fuel cell is unable to provide the necessary power to the motor.
- An adaptive controller based on a linear model that adjusts the hydrogen flow into the fuel cell in response to changing power demand.
- A thermal controller based on a nonlinear model that regulates the temperature of the fuel cell.

The design of these controllers is described in the sections below.

3. SWITCHING CONTROLLER DESIGN

There has been considerable research effort in modeling fuel cells [Nguyen and White, 1993]. In electric and fuel cell vehicles the battery is charged and discharged continuously and so knowledge of the transient behavior of the batteries is very important. Dynamic models developed from electrochemical principles like the cell sandwich model give spatial distribution of potentials and chemical compositions inside the cell as well as the transient behavior of cell potential and temperature. However for control oriented studies we require models which can be simulated quickly. Equivalent electric circuit models have been developed in the literature which give an accurate prediction of state-of-charge (SOC) of the battery [He and Hodgson, 2002].

He and Hodgson [2002] have observed that while discharging a battery over a period of time there exists a cutoff or critical voltage beyond which the battery performance deteriorates rapidly as the voltage begins to fall rapidly. To avoid operation near the critical voltage the state of charge is set to zero at the cutoff voltage and is defined as

$$SOC = 1 - \frac{Voc_{cutoff}}{Voc_{full}} \tag{1}$$

where Voc_{full} is the voltage of the battery at full capacity and Voc_{cutoff} is the battery terminal voltage at the critical point. Practically, it is difficult to measure the open circuit voltage at each instant hence utilizing the relationship between the SOC and the available battery capacity SOC can be redefined as

$$SOC = 1 - \frac{UsedCapacity}{TotalCapacity} \tag{2}$$

The total current drawn from the battery can be used as an indicator for the used capacity and is given by.

$$CAP_{used} = \int_0^t I.dt \tag{3}$$

So now the SOC is one when the battery is fully charged and zero when discharged to the critical voltage. It is desirable to maintain the SOC around 0.5-0.7.

A battery model which requires experimentally obtained open-circuit voltage and battery resistance data and predicts the battery terminal voltage, current, and SOC as a dynamic function of operator imposed power demand has been developed based on the model by He and Hodgson [2002]. The model consists of the battery as an ideal voltage source with an internal resistance. This battery model is characterized by the idealized open circuit voltage, V_{oc}, and the internal battery resistance, R_b. The terminal voltage can be expressed in terms of V_{oc} and R_b as

$$V_{term} = V_{oc} - I * R_b \tag{4}$$

The terminal voltage of a battery during discharge is lower than the instantaneous open circuit voltage because of the internal resistance inside the battery. Hence current I is given a positive sign when the cell is discharging. Similarly when the cell is charging we need to apply a voltage greater than the V_{oc} to overcome the internal resistance inside the cell so the current in this case is chosen to be negative.

The open circuit voltage and the internal resistance of the battery are both functions of SOC and temperature. For a battery operating at constant temperature the relationship between V_{oc}, Rb and the SOC can be determined experimentally.

The power available at the terminals of the battery is given by the product of voltage and current and substituting the expression for voltage from equation 4. we have

$$Pwr_{term} = V_{term}I = IV_{oc} - I^2 * R_b \tag{5}$$

For a particular power demand we can calculate the current by solving equation 5 which is a quadratic equation in I.

$$I = \frac{V_{oc} - \sqrt{(V_{oc}^2 - 4.R_b.Pwr)}}{2R_b} \tag{6}$$

where Voc and Rb are both functions of the SOC. The same sign convention as was used for the current is used i.e. the power is positive during discharge and negative during charge. The current calculated from eq. 6 is used to calculate the used capacity from eq. 3, which in turn is used to calculate the SOC by eq. 2. The V_{oc} and R_b are obtained for the new SOC from the experimental data. Using the new values of V_{oc} and R_b the current is estimated using eq. 6.

The switching controller is a logic based on-off controller that switches back and forth between the fuel cell and the battery to meet the power demand. As discussed earlier there is a time lag between the methane entering the reformer and the hydrogen coming out of the fuel processor. If the power demand remains constant the power produced by the fuel cell is sufficient to meet the power demand. The actual power demand curve is not a straight line and has a lot of fluctuations. To meet this fluctuating power demand, the fuel cell may switch to the battery. The switching controller has to address the following scenarios:

- *Increase in Power Demand*: Whenever there is an increase in power demand the fuel cell cannot produce the required power (P_r) because of the time delay (τ) in producing power and hence any deficit in power demand is handled by switching to the battery until the fuel cell can produce sufficient power. During this time delay the power produced by the battery is
$$P_{bat} = P_r - P_{fc} \quad for \quad t < \tau \tag{7}$$
- *Decrease In Power Demand*: During deceleration or decrease in power demand the fuel cell continues to produce the power requested until the time delay has elapsed. This excess power produced by the fuel cell during decrease in power demand should be routed to the battery, so that the battery can be charged. The same equation used in the scenario above can be used here. Since here the power requested is less than the power produced by the fuel cell the P_{bat} is negative which indicates that the battery is being charged.
- *State of Charge*: The state of charge of the battery should be always maintained above a specified target(SOC_{target}). But during sudden increase in power demand the battery might be discharged rapidly and the SOC might fall below the specified target and also the initial SOC itself might be less than the SOC_{target}. When the SOC of the battery falls below SOC_{target} the controller should direct the fuel cell to produce power to charge the battery in addition to the power demand.
$$P_{fc} = P_r + P_{bat} \quad if \quad SOC < SOC_{target} \tag{8}$$
- *Total Power Demand*: Since the fuel processor and the fuel cell system were designed for a maximum power output of 50 kW, the switching controller should make sure that the power demand from the fuel cell is not greater than 50 kW.

The fuel processor, fuel cell system and battery model along with the switching controller were simulated in MATLAB for different power demands. For a simple case where the power demand is a step increase followed by a step decrease the power profiles are given in Figure 2. Notice that the fuel cell supplies the power with a time delay of 4 seconds in the meantime the battery supplies the requested power demand. Once the fuel cell is able to meet the power demand the battery is turned off until 15 seconds at which time the battery again is used to supply the necessary power demand. At 30 seconds when there is a decrease in power demand the deficit power is sent to the battery to charge it until the fuel cell reaches the level of the new power demand.

To get a more realistic power vs time profile we obtained the power profile for a small car from an existing speed vs time profile using ADVISOR software package [NREL, 2002]. The Urban Dynamometer Driving schedule (UDDS) which is designed for light duty vehicle testing in city driving conditions has been used. The speed versus time profile is shown in Figure 3. The profiles of power requested, fuel cell power and battery power versus time are plotted in Figure 4.

The power supplied by the battery also depends on the initial SOC of the battery. For the same cycle the system was simulated for different initial SOC as shown in Figure 5. The controller was designed to maintain the SOC above

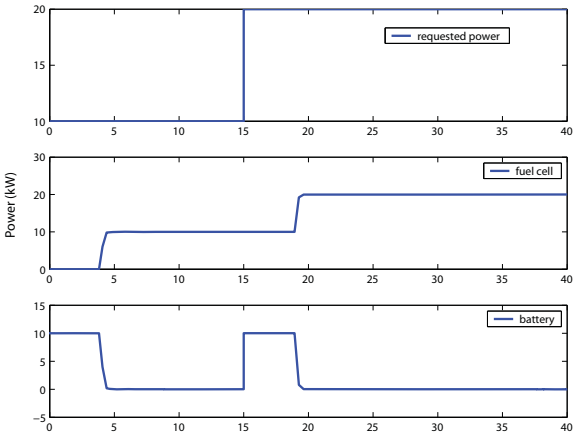

Fig. 2. Power profile

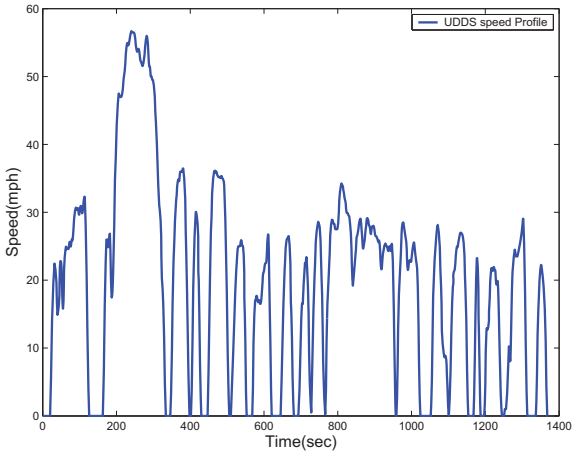

Fig. 3. Speed Vs time profile for UDDS

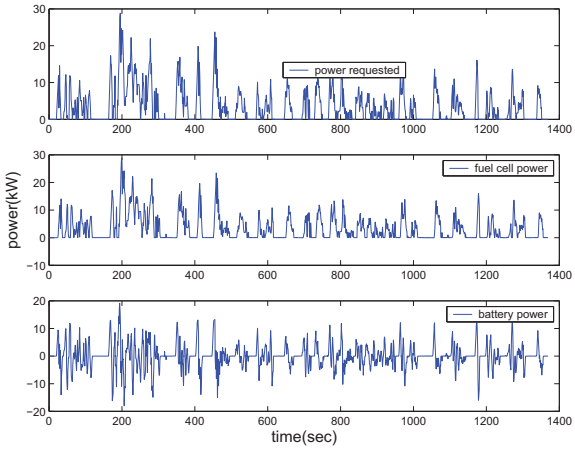

Fig. 4. Power profiles for the UDDS

0.5. For the initial conditions where the battery is almost charged (SOC=0.9) and semi charged (SOC=0.64) the profiles look similar. But for the case where the initial SOC is less than 0.5 the controller is activated and brings the SOC level to above 0.5.

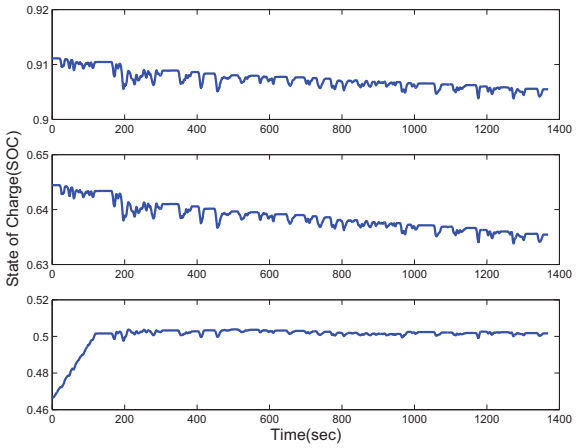

Fig. 5. State of charge for different initial conditions

Current battery technology in hybrid vehicles involves the use of nickel metal hydride (NiMH) battery packs. For instance, the Toyota Prius consists of 38 prismatic modules of a new generation NiMH design with a total pack nominal voltage of 273.6 V and a total energy capacity of 1.8 kWh [Kelly *et al.*, 2001]. The dimensions of this battery pack are 19.6 mm x 106 mm x 275 mm (volume of 57 l). The battery considered in this paper is of the same order of magnitude with a peak voltage of 300 V. If we assume that the energy capacity of the battery is 1.8 kWh (same as the Prius battery) and the battery has to have a state of charge of at least 50%, this battery would deliver 50 kW for 1 minute starting from a fully charged state before depleting to 50%. Thus, from a cold start, the reformer would have to be operational within 1 minute so that the car can switch from the battery to the fuel cell. It was shown in the previous section that once the fuel cell is operational, under realistic city driving conditions, the charge of the battery never goes under 50%. Newer gas-electric and fuel cell-electric hybrid vehicles use lithium ion battery technology. These batteries have superior power density versus energy density characteristics when compared to either NiMH batteries or supercapacitors. The second generation Honda Clarity fuel cell-electric hybrid is equipped with such a battery module. It is rated for 283 volts, and replaces the super capacitor energy storage system of the first generation Clarity. Improvement in lithium ion battery technology is ongoing. Current research indicates that energy capacity of 6-18 kWh are achievable with a calendar life of 15 years and 2500-5000 charge depleting cycles [Axsen *et al.*, 2008]. Preliminary research on magnesium ion battery systems suggest another order of magnitude in performance improvent is achievable [Axsen *et al.*, 2008].

4. ADAPTIVE CONTROLLER DESIGN FOR POWER GENERATION SUBSYSTEM

Pukrushpan [2003] developed and experimentally verified a dynamic model for a PEM fuel cell stack system similar to the one shown in Fig. 1. The model incorporates transient behavior that is important for controller design and analysis. In particular, a time-scale analysis of the various components was conducted and dynamic balances were developed for those operations that relate to automobile operations. Slower dynamics associated with temperature regulation and heat dissipation were ignored. Inertia dynamics along with nonlinear curve fitting of the compressor characteristic map were used to model the compressor. The manifold dynamics were based on lumped-volume filling dynamics. Static models of the air cooler and air humidifier were developed from thermodynamic relations. The fuel cell stack model was composed of four interacting submodels, namely stack voltage, cathode flow, anode flow and membrane hydration. The dynamic equations at the cathode and anode were developed using mass conservation principles and thermodynamic and psychometric properties of air. All gases were assumed to behave like an ideal gas. Spatial variations in temperature and concentration were ignored. It was assumed that the anode inlet flow rate could be instantaneously adjusted by a valve to maintain the minimum pressure difference between the cathode and the anode. Mass transport of water across the fuel cell membrane was calculated in membrane hydration model. Both water content and mass flow were assumed to be uniform over the surface of the membrane. However, this model developed by Pukrushpan [2003] consists of a large number of coupled, nonlinear differential and algebraic equations (DAE) and adaptive control theory cannot be applied directly to this system.After suitable substitution of variables, we obtained a reduced model of the fuel cell system that is a set of nine ordinary differential equations and is suitable for controller design and analysis [Kolavennu *et al.*, 2008]. In this model, it is assumed that all the cells in the stack perform similarly, i.e., by analyzing the polarization curve of a single cell, the stack performance can be estimated. The power from the fuel cell, which is a function of the current and voltage, is given by:

$$P = V_{st} I = (N_c V_c)(i A_c) \tag{9}$$

where P is the power produced by the fuel cell, V_{st} is the voltage of the stack which is the product of the number of cells N_c and the individual cell voltage V_c, I is the current drawn from the cell and is the same for each cell and depends on the area of cross section A_c, i is the current density.

The reversible standard potential E^o for the above cell reaction is 1.23 V at 25 ^oC as determined from the change in the Gibb's free energy. The actual voltage depends upon the concentration of the species and temperature at which the fuel cell is operating. The concentration dependence is given by the Nernst equation [Pukrushpan, 2003] as shown below:

$$\begin{aligned} E \;=\; & 1.229 - 8.5 \times 10^4 (T_{fc} - 298.15) + \\ & 4.3085 \times 10^{-5} T_{fc} \left[ln(P_{H_2}) - \frac{1}{2} ln(P_{O_2}) \right] \end{aligned} \tag{10}$$

where E is the open circuit voltage, the fuel cell temperature T_{fc} is in K, and reactant partial pressures P_{H_2} and P_{O_2} are expressed in atm. The actual cell voltage at any given current density is obtained by subtracting the activation, ohmic and concentration losses from the reversible potential as expressed below.

$$\nu_{fc} = E - \nu_{act} - \nu_{ohm} - \nu_{conc} \tag{11}$$

where ν_{act}, ν_{ohm} and ν_{conc} are activation, ohmic and concentration overvoltages. These losses are a function of the current density, pressure, membrane humidity and

also on the type of membrane and are represented by the empirical equations given below

$$\nu_{act} = \nu_0 + \nu_a(1 - e^{10i}) \tag{12}$$

$$\nu_{ohm} = i.R_{ohm} \tag{13}$$

$$\nu_{conc} = i\left(c_2 \frac{i}{i_{max}}\right)^2 \tag{14}$$

where ν_0, ν_a and c_2 are functions of temperature, pressure and membrane humidity of the cell. Using this model we can calculate the power produced by the fuel cell based on the voltage current characteristics. For a given current demand the voltage is calculated using Eq. 11 and thereby the power output of the fuel cell.

For the fuel cell systems to operate at levels comparable to existing internal combustion engines, the key issue that should be addressed is the *transient* behavior of fuel cell systems. Automobiles are subjected to significant load transitions during operation and the fuel cell system should be able to produce power which can follow this varying load profile. Power produced by the fuel cell is dependent on the voltage current characteristics. The transient response data from the nonlinear model presented in [Kolavennu *et al.*, 2008] was generated by subjecting the nonlinear system to a series of step inputs in the current around the 100 Amperes operating point. Utilizing this input output data from the nonlinear model system identification techniques were employed to derive a linear second order model was fit between the current demand and the voltage produced by the fuel cell stack. The transfer function G_p is given below

$$G_p = \frac{-390.78}{s^2 + 27.291s + 2068.8} \tag{15}$$

This transfer function is used in this paper to design an adaptive controller to regulate the power output of the fuel cell to the power demand. This adaptive controller is then implemented on the *nonlinear* model described in [Kolavennu *et al.*, 2008]. The control problem is to track the power demand of the motor using current as the manipulated variable.

To get a more realistic power vs time profile we obtained the power profile for a small car from an existing speed vs time profile using ADVISOR software package [NREL, 2002]. The Urban Dynamometer Driving schedule(UDDS) which is designed for light duty vehicle testing in city driving conditions was used.

Model reference adaptive control (MRAC) is derived from the model reference control (MRC) problem. The objective of MRC is to find the feedback control law that changes the structure and dynamics of the plant so that its I/O properties are exactly the same as those of a reference model. The structure of an MRC scheme for a LTI, SISO plant is shown in Fig. 6 [Ioannou and Sun, 1996]. Here, $W_m(s)$ is the transfer function of the reference model, $r(t)$ a given reference input signal, $y_m(t)$ the output of the reference model and $y(t)$ is the plant output. The feedback controller, denoted by $C(\Theta_c)$, is designed so that all signals are bounded and the closed-loop plant transfer function from r to y is equal to $W_m(s)$. This transfer function matching guarantees that for any given reference input $r(t)$, the tracking error $e = y - y_m$, which represents the

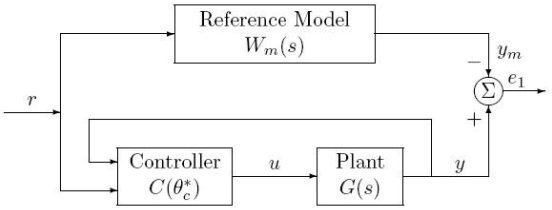

Fig. 6. Model Reference Adaptive Control

Table 1. Performance of MRAC on different road profiles

Profile or Cycle	ITAE error
UDDS	40.5
Federal Test Procedure	42.76
US06	55.13
Highway Fuel Economy Test	11.09
Extra Urban Driving Cycle	8.20
Indian Highway Profile	10.20

deviation of the plant output from the desired trajectory ym, converges to zero with time.

The model reference is chosen to be:

$$W_m = \frac{1}{s + 0.023} \tag{16}$$

The performance of the adaptive controller can be improved by adding some derivative action, i.e., using a PD controller in conjunction with the adaptive controller. This essentially makes the linearized plant represented by eq. 15 of unity relative degree which is the same as that of the reference model eq. 16.

The Environmental Protection Agency (EPA) reviews and revises as necessary the regulations governing the Federal Test Procedures (FTP) to insure that vehicles are tested under circumstances which reflect the actual current driving conditions under which motor vehicles are used, including conditions relating to fuel, temperature, acceleration, and altitude. The adaptive controller was tested on a variety of profiles. The controller was designed for the UDDS profile using the linearized model represented by eq. 15 and the same settings were employed for the remaining profiles. The resulting adaptive controller was implemented on the *nonlinear* model given in [Kolavennu *et al.*, 2008]. The Integrated Time Averaged Error (ITAE) was computed for each power profile. The results are shown in Table 1. It is observed that the adaptive controller with derivative action is able to track power profiles resulting from a wide variety of road conditions. A PID tuning procedure for the UDDS profile resulted in an ITAE error of 91.46. However, this controller when implemented on the US HWY profile resulted in loss of stability. On the other hand, the adaptive controller that was designed for the UDDS profile was able to successfully track the Federal Test Procedure profile, the US06 profile, the Highway Fuel Economy Test profile, the Extra Urban Driving Cycle profile, and the Indian Highway profile with no off-line tuning.

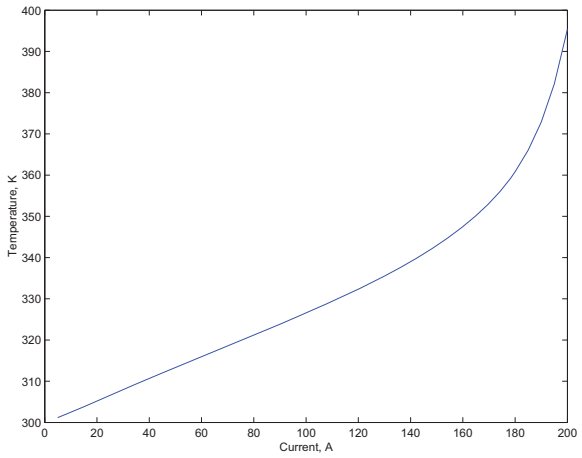

Fig. 7. Steady State Temperature versus Current in Fuel Cell

5. THERMAL CONTROLLER FOR FUEL CELL TEMPERATURE REGULATION

In this section, a dynamic model is developed that accounts for temperature changes in a PEM fuel cell. The dynamic model is obtained by extending a static current-voltage description to include temperature difference and by dynamically modeling the stack temperature. The following chemical reaction occurs in the fuel cell:

$$2H_2 + O_2 \rightarrow 2H_2O \tag{17}$$

The accumulation term for each species is negligible in the fuel cell compared to the mass of the fuel cell stack. Thus, a steady state model can be assumed for the gaseous and liquid species as follows:

$$\dot{N}_{i,out} = \dot{N}_{i,in} + \nu_i \dot{\xi} \tag{18}$$

where $\dot{N}_i$ is the molar flow rate of species i, ν_i is the stoichiometric coefficient and $\dot{\xi}$ is the reaction rate. It can be shown that this steady state assumption leads to the following dynamic balance for the temperature of the fuel cell stack:

$$m_{fc} C_{p_{fc}} \frac{dT_{fc}}{dt} = -C_p^* I(T_{fc} - T_\infty) - \Delta\tilde{H} I - hA(T_{fc} - T_\infty) - VI \tag{19}$$

where m_{fc} is the mass of the fuel cell stack, $C_{p_{fc}}$ is the specific heat of the fuel cell stack, C_p^* is the mole average specific heat of the reacting species, and T_∞ is the ambient temperature.

This provides a dynamic relation between the stack temperature, current and voltage. Fig. 7 shows the steady state relationship between temperature and current at a humidity of 50% in the cell. It is observed that the cell temperature increases nearly linearly with current until the design point (167 A), which is at optimum power output, and then increases rapidly due to cell inefficiency. The above equation was integrated numerically with realistic operating conditions of the fuel cell system and it was observed that the temperature dynamics are very slow compared to the dynamics of the fuel cell. In particular, it takes about 50 minutes to go from a cold start to the steady state temperature when the current is 150 A.

We are currently developing a nonlinear controller that utilizes the above model to regulate temperature to the desired set-point in the face of fluctuating power demand.

REFERENCES

Axsen, J., Burke, A., and Kurani, K., "Batteries for Plug-in Hybrid Electric Vehicles (PHEVs): Goals and the State of Technology circa 2008," *UCD-ITS-RR-08-14*, 2008

He, X. and Hodgson, J.W., " Modeling and Simulation for Hybrid Electric Vehicles: Modeling." *Intelligent Transportation Systems*, volume 3, 235-243, (2002)

Ioannou P. and J. Sun, *Robust Adaptive Control*, Prentice Hall, Inc., 1996

Kelly, K.J., Mihalic, M., and Zolot, M., "Battery Usage and Thermal Performance of the Toyota Prius and Honda Insight during Chassis Dynamometer Testing," *NREL/CP-540-31306*, 2001

Kolavennu, P.K., Telotte, J.C., and Palanki, S., "Design of a Fuel Cell Power System for Automotive Applications," *Int. J. Chemical Reactor Engng*, Vol 4: A19 (2006)

Kolavennu, P.K., Palanki, S., Cartes, D.A. and Telotte, J.C., "Adaptive Controller for Tracking Power Profile in a Fuel Cell Powered Automobile," *J. Process Control*, 18, 558-567 (2008)

Nguyen, T.V., and White, R.E., "A Water and Heat Management Model for Proton-exchange-membrane Fuel Cells," *J. Electrochem. Soc.*, 140, 8, 2178-2186 (1993)

National Renewable Energy Laboratory, "ADVISOR (Advanced Vehicle Simulator)", 2002

Pukrushpan, J. T., *Modeling and Control of Fuel Cell Systems and Fuel Processors*, PhD thesis, The University of Michigan, Ann Arbor, 2003

Zalc, J.M., and Loffler, D.G., "Fuel processing for PEM fuel cells: transport and kinetic issues of system design," *J. Power Sources*, 111, 58-64 (2002)